Charged multivesicular body protein 4C promotes the progression of cervical cancer through the HPV E6/miR-543 axis

REN-CI LIU[1-5*], YU-MENG JI[1-5*], JING HUANG[1-5], YU-PING DU[1-5], YU-MIN ZHONG[1-5] and XIU-JIE SHENG[1-5]

[1]Department of Obstetrics and Gynecology, The Third Affiliated Hospital Guangzhou Medical University, Guangzhou, Guangdong 510150, P.R. China; [2]Department of Gynecology, The Third Affiliated Hospital Guangzhou Medical University, Guangzhou, Guangdong 510150, P.R. China; [3]Guangdong Provincial Key Laboratory of Major Obstetric Diseases, The Third Affiliated Hospital Guangzhou Medical University, Guangzhou, Guangdong 510150, P.R. China; [4]Guangdong Provincial Clinical Research Center for Obstetrics and Gynecology, The Third Affiliated Hospital Guangzhou Medical University, Guangzhou, Guangdong 510150, P.R. China; [5]Guangdong-Hong Kong-Macao Greater Bay Area Higher Education Joint Laboratory of Maternal-Fetal Medicine, The Third Affiliated Hospital Guangzhou Medical University, Guangzhou, Guangdong 510150, P.R. China

Received July 17, 2024; Accepted February 21, 2025

DOI: 10.3892/ol.2025.15021

Abstract. Charged multivesicular body protein 4C (CHMP4C), as a subunit of endosomal sorting complex required for transport-III, is important for the abscission checkpoint in cell division, preventing premature cell division and genetic damage. The present study aimed to assess the role of CHMP4C in cervical cancer and the associated mechanisms. The levels of CHMP4C in normal and cervical cancer tissues were detected by immunohistochemistry. The MTT assay, apoptosis, wound-healing assay, and cell invasion assay were performed. Western blotting was performed to analyze the level of cancer-related proteins following CHMP4C downregulation and the CHMP4C expression following E6 downregulation and miR-543 upregulation. The transfection effectiveness of siRNA, plasmid, and miRNA mimic as well as the expression of miR-543 after silencing E6 were assessed by RT-PCR. The dual-luciferase reporter assay was used to demonstrate a connection site between CHMP4C and miR-543. The results demonstrated that CHMP4C expression in cervical cancer tissues was significantly higher than that in normal tissues. Furthermore, downregulation of CHMP4C expression significantly reduced the proliferation, migration and invasion of cervical cancer cells and significantly increased the rate of apoptosis compared to the si-scramble group. Comparison with the si-scramble group, silencing CHMP4C expression also significantly reduced the expression of Bcl2, Bcl-xL and Survivin, and was associated with a significant increase in Caspase-7 expression. After the knockdown of human papillomavirus (HPV)-encoded E6, in comparison to the si-scramble group, microRNA (miR)-543 expression was significantly elevated and CHMP4C expression significantly decreased. Moreover, a connection site was detected between miR-543 and CHMP4C. These findings indicate that CHMP4C accelerates the tumorigenesis and progression of cervical cancer through the HPV E6/miR-543 axis.

Correspondence to: Professor Xiu-jie Sheng, Department of Gynecology, The Third Affiliated Hospital Guangzhou Medical University, 63 Duobao Road, Liwan, Guangzhou, Guangdong 510150, P.R. China
E-mail: 1815260097@qq.com

*Contributed equally

Abbreviations: CHMP4C, charged multivesicular body protein 4C; GEPIA, Gene Expression Profiling Interactive Analysis; HPV, human papillomavirus; miRNA/miR, microRNA; siRNA, small interfering RNA; 3'-UTR, 3'-untranslated region; IAP, inhibitor of apoptosis proteins

Key words: cervical cancer, HPV E6, CHMP4C, miR-543, tumorigenesis, cancer progression

Introduction

Cervical cancer accounts for a considerable proportion of gynecological malignancies. Cervical cancer ranked fourth among female cancer-related morbidity and mortality, with 661,021 new cases and 348,189 deaths in 2022 (1). According to GLOBOCAN 2022, cases in China accounted for 22.7% and 16.0% of global morbidity and mortality rates, respectively, with 150,659 new cases and 55,694 deaths (2). In addition, due to the low population coverage rate (21.4%) for cervical cytology and the low human papillomavirus (HPV) vaccination rate, eliminating cervical cancer is a challenging task (3). Currently, cervical cancer is treated with a comprehensive conventional approach that includes surgery, radiotherapy and chemotherapy (4). However, this strategy is not effective in patients with advanced cancer, and there is a high incidence of recurrence and metastasis. The 5-year disease-free survival is approaches 100% for patients with stage IA cervical cancer, 70-85% for those with stage IB1 and smaller IIA lesions, 50-70% for those with stages IB2 and IIB, 30-50% for those with stage III, and 5-15% for those with stage IV (5). Therefore,

it is important to elucidate the mechanisms of cervical cancer development and identify specific tumor markers.

It has been established that the activation of proto-oncogenes and the inactivation or mutation of tumor suppressor genes are involved in the tumorigenesis of cancer (6). Therefore, genes related to cervical cancer were screened out using the Gene Expression Profiling Interactive Analysis (GEPIA) database. CHMP4C, as a subunit of endosomal sorting complex required for transport-III, is essential for the Aurora B-mediated abscission checkpoint (NoCut) and can delay the abscission time and reduce the accumulation of DNA damage (7,8). A previous study also reported that CHMP4C is undetectable in normal tissues but overexpressed in ovarian cancer tissues (9). Moreover, there are higher expression levels of CHMP4C in the extracellular vesicles of prostate cancer with a high Gleason score, which may promote the progression of prostate cancer (10). However, the relationship between CHMP4C and cervical cancer remains to be studied. Therefore, the present study aimed to assess the role of CHMP4C in the development of cervical cancer and evaluate the regulatory pathways in which CHMP4C may be involved.

Materials and methods

Bioinformatics analysis. GEPIA (gepia.cancer-pku.cn/index.html) was used to screen genes overexpressed in cervical squamous cell cancer, developed survival curve, and automatically calculate Log-rank and HR. Additionally, targetscan (https://www.targetscan.org/vert_72/), mirDIP (http://ophid.utoronto.ca/mirDIP/), and miR-Gator (http://mirgator.kobic.re.kr/), to suggest miRNA with binding sites to target genes.

Specimens. The present study obtained 19 normal cervical tissues, 88 cervical squamous cell carcinoma tissues and 8 cervical adenocarcinoma tissues from hospitalized patients in the Third Affiliated Hospital Guangzhou Medical University (Guangzhou, China) between 2014-2019. Patients diagnosed with metastatic cervical cancer or other malignant tumors, or with a history of radiotherapy and chemotherapy before surgery were excluded. The patients agreed to use the tissue removed during surgery for general scientific research and signed an informed consent form. The Ethics Committee of the Third Affiliated Hospital Guangzhou Medical University approved the present study (approval no. 2019-037). The tissues were scored according to the degree of staining and the percentage of positively stained cells, and the final scores were added.

Cell culture. The HPV16-positive cervical cancer SiHa cell line (National Infrastructure of Cell Line Resource) was cultured in RPMI1640 medium (HyClone; Cytiva), and the human cervical epithelial immortalized H8 (Jennio Biotech Co., Ltd.), HPV16-positive cervical cancer Caski (National Infrastructure of Cell Line Resource) and HPV18-positive cervical cancer HeLa (Pricella®; Wuhan Elabscience Biotechnology Co., Ltd.) cell lines were cultured in DMEM medium (HyClone; Cytiva), containing 10% fetal bovine serum (Shanghai Excell Biological Technology Co., Ltd.). The cells were plated in petri dishes and cultured in an incubator at 37˚C and 5% CO_2 atmosphere.

Small interfering (si)RNA transfection. siRNAs (Sigma-Aldrich; Merck KGaA) against target genes were used to knockdown the expression of the target genes, and Lipofectamine™ 3000 (Thermo Fisher Scientific, Inc.) was used as a cell transfection reagent. A total of 50 nM siRNA was transfected into SiHa and HeLa cells at 37˚C for 48 h immediately before subsequent experiment. The target genes and corresponding siRNA sequences were as follows: CHMP4C, 5'-CAGAUUGAUGGCACACUUUdTdT-3' (forward) and 5'-AAAGUGUGCCAUCAAUCUGdTdT-3' (reverse); HPV16 E6, 5'-GAGUAUAGACAUUAUUGUUdTdT-3' (forward) and 5'-AACAAUAAUGUCUAUACUCdTdT-3' (reverse); and HPV18 E6, 5'-CAGACUCUGUGUAUGGAGAdTdT-3' (forward) and 5'-UCUCCAUACACAGAGUCUGdTdT-3' (reverse). The scrambled siRNA sequences used for the control were as follows: 5'-UUCUCCGAACGUGUCACGUTTdTdT-3' (forward) and 5'-ACGUGACACGUUCGGAGAATTdTdT-3' (reverse).

Plasmid and mimics transfection. Full-length cDNAs of human CHMP4C were synthesized by Guangzhou Dahong Biotechnology Co., Ltd. and cloned into the expression vector pCMV-MCS-3Flag (Guangzhou Dahong Biotechnology Co., Ltd) (Fig. 1). When cell confluence reached 80-90%, the plasmids were transfected using Lipofectamine 3000 and p3000 reagents (Thermo Fisher Scientific, Inc.), following the manufacturer's protocol. A total of 50 nM microRNA (miRNA/miR) and negative control mimics (Guangzhou RiboBio Co., Ltd.) were transfected into SiHa and HeLa cells using Lipofectamine 3000 reagent. A total of 48 h after transfection at 37˚C, the transfection efficiency was immediately assessed using reverse transcription-quantitative PCR (RT-qPCR). The sequences of the miR-543 mimic were 5'-AAACAUUCGCGGUGCACUUCUU-3' (sense), 5'-UUUGUAAGCGCCACGUGAAGAA-3' (antisense). The sequences of the negative control mimic were 5'-UUUGUACUACACAAAAGUACUG-3' (sense), 5'-AAACAUGAUGUGUUUUCAUGAC-3' (antisense).

MTT assay. After the SiHa and HeLa cells were digested and collected, $3x10^3$ cells and 100 μl medium were added to each well in a 96-well plate. After the cells had adhered, the experimental group was transfected with CHMP4C siRNA, whereas the negative control group was transfected with scramble siRNA. A total of 20 μl MTT solution was then added to each well, followed by incubation at 37˚C for 4 h. The liquid was then aspirated from the well, and 150 μl dimethyl sulfoxide was added. Finally, a microplate reader (BioTek; Agilent Technologies, Inc.) was used to measure the optical density value of each well at 490 nm.

Wound-healing assay. SiHa and HeLa cells were inoculated in a six-well plate. When the cell density reached ~80%, a 200 μl pipette tip was used to scratch the cells, and then serum-free medium was added. Images of the scratches were captured under a microscope (Olympus IX73; fluorescence microscope; Olympus Corporation and Leica DMi1; light microscope; Leica Microsystems GmbH) and then processed using cellSens Version 2.1 (Olympus Corporation) and Leica Application Suite X Version 4.12 software (Leica Microsystems GmbH). The wound area was measured using Image J software

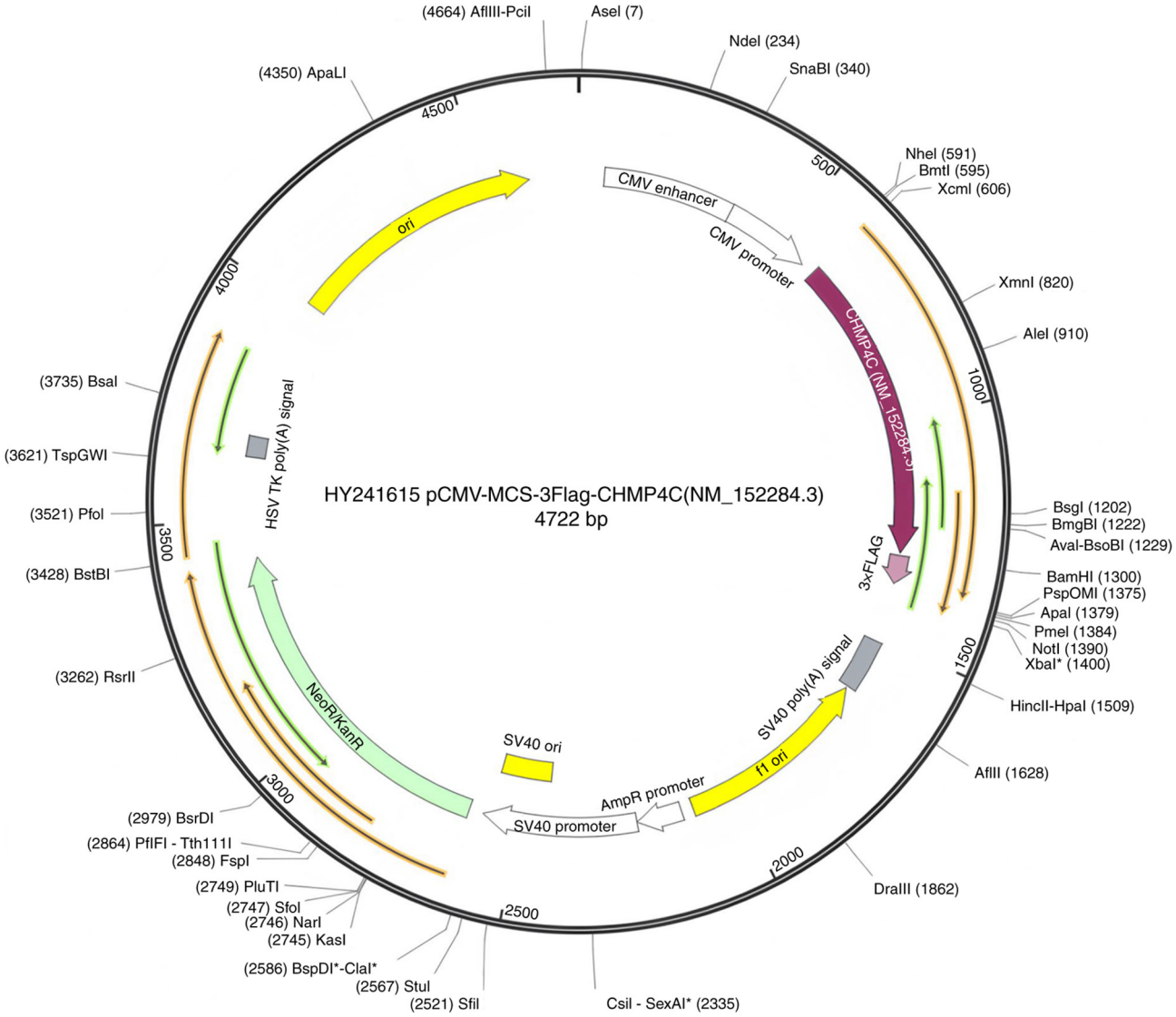

Figure 1. CHMP4C plasmid. Full-length cDNAs of human CHMP4C were cloned into the expression vector pCMV-MCS-3Flag.

Version 1.52a (National Institutes of Health). The following formula was used to assess the level of wound-healing: Mobility=(starting area-final area)/starting area x100%.

Apoptosis assay. The transfected SiHa and HeLa cells were collected using EDTA-free trypsin and washed once with PBS. The cells were resuspended in 100 μl binding buffer (1X) and 5 μl Annexin V-FITC/PI staining solution (BD Biosciences) and placed in the dark. After the addition of 400 μl binding buffer (1X) to each tube, apoptosis was detected using flow cytometry (BD FACScanto™ II Clinical Flow Cytometry System; BD Biosciences, and Attune NxT Flow Cytometer; Thermo Fisher Scientific, Inc.). FlowJo software (version 10.8; BD Biosciences) and Attune NxT Flow Cytometry Software (version 2.6; Thermo Fisher Scientific, Inc.) were used for analysis.

Cell invasion assay. Matrigel (BD Bioscience) was diluted at a 1:15 ratio with cold serum-free medium (RPMI-1640 or DMEM; HyClone; Cytiva) refrigerated at 4˚C and 30 μl was plated into the filters of the Transwell chambers (Corning, Inc.). Then the chambers were placed in a 24-well plate in a 37˚C incubator for 4 h. Cells were suspended at a density of $4x10^4$ in 200 μl serum-free medium (RPMI1640 or DMEM, HyClone; Cytiva) and plated in the upper chamber, whilst 600 μl medium supplemented with 10% fetal bovine serum (Shanghai Excell Biological Technology Co., Ltd. Bio) was added to the lower chamber. After incubation at 37˚C for 48 h, the chamber was fixed with 4% formaldehyde for 30 min and stained with 1% crystal violet for 15 min both at room temperature. Photographs were captured under a microscope (Olympus IX73, fluorescence microscope, Olympus Corporation), and the invasive cells were manually counted. Each experiment was performed in triplicate, and images of 3 fields of view were captured for each replicate.

Immunohistochemistry. The normal and cervical cancer tissues were fixed in 4% paraformaldehyde (at room temperature for 24 h, embedded in paraffin wax, and cut into 4 mm slices. The paraffin-embedded tissue sections were heated in a 65˚C incubator for 4 h and dewaxed with xylene (Foshan Bodi Chemical Reagent Co., Ltd) for 20 min twice at room temperature. Then they were immersed into 100% alcohol (Foshan

Bodi Chemical Reagent Co., Ltd) for 5 min, 95% alcohol for 2 min, 85% alcohol for 2 min, 75% alcohol for 1 min, and finally turned into distilled water for 3 min 3 times, so as to fully hydrate. The sections were immersed in an EDTA antigen retrieval solution and heated in a pressure cooker for 5 min with the cover unlocked. Then the cooker was locked, removed from the heat source 3 min after the pressure reaches the highest. After then, the sections allowed to cool at room temperature. After inactivation of endogenous catalase activity using 3% hydrogen peroxide, the sections were blocked with 5% BSA (BEIJING SOLARBIO Technology Co., Ltd.) in a 37˚C incubator for 40 min. The sections were then incubated with anti-CHMP4C antibodies (1:400; #GTX122876; GeneTex, Inc.) overnight at 4˚C. The following day, the sections were re-warmed at room temperature for 30 min and washed three times with PBS. Horseradish peroxidase-conjugated anti-rabbit antibodies (1:800; cat. no. ab97051; Abcam) were then added and the sections were incubated for 45 min in a 37˚C incubator. After diaminobenzidine coloration and hematoxylin staining at room temperature for 10 min, the sections were dehydrated, sealed with a neutral resin and imaged under a microscope (Leica Microsystems GmbH).

Dual-luciferase reporter assay. As the presence of a binding site between CHMP4C and miR-543 was predicted (data not shown), a CHMP4C 3'-untranslated region (3'-UTR) containing a miR-543-binding site sequence was designed. 293T cells (Pricella®; Wuhan Elabscience Biotechnology Co., Ltd.) were seeded into 24-well plates and transfected with 600 ng SV40-dual-luciferase vector (Shanghai Genechem Co., Ltd.) expressing a wild type CHMP4C 3'-UTR using Lipofectamine™ 3000 (Thermo Fisher Scientific, Inc.), whilst the mutant type acted as a control. At the same time, 50 nM miR-543 or negative mimics (Shanghai Genechem Co., Ltd.) were co-transfected. The sequence of the miR-543 mimics were 5'-AAACAUUCGCGGUGCACUUCUU-3' (sense) and 5'-AAGAAGUGCACCGCGAAUGUUU-3' (antisense). The sequences of the negative control mimic were 5'-UUUGUACUACACAAAAGUACUG-3' (sense), 5'-AAACAUGAUGUGUUUUCAUGAC-3' (antisense). After 48 h, the Dual-Luciferase® Reporter Assay System (Promega Corporation) was used to detect the level of luciferase activity. The relative luciferase intensity was normalized to renilla luciferase activity.

RT-qPCR. Total RNA was extracted from SiHa and HeLa cervical cancer cells using the TRIzol reagent (Takara Bio, Inc.). After separation, precipitation, washing and dissolution, the concentration of RNA was detected using a spectrophotometer [Unico (Shanghai) Instrument Co., Ltd.]. For mRNA analysis, 2 μg total RNA was reverse-transcribed to synthesize complementary (c)DNA using random primers and avian myeloblastosis virus transcriptase (PrimeScript™ RT reagent Kit (Perfect Real Time); Takara Bio, Inc.). The reverse transcription program was set at 37˚C for 15 min, 85˚C for 5 min, and finally cooled to 4˚C. qPCR amplification of the cDNA was then performed using the SYBR® Premix Ex Taq™ II kit (Takara Bio, Inc.) with 18S as an internal control. The amplification conditions were as follows: Initial denaturation at 95˚C for 30 s, followed by 40 cycles of 95˚C for 5 s and an 60˚C for 30 sec. The Hairpin-it™ miRNAs qPCR Quantitation Kit (Shanghai GenePharma Co., Ltd.) was used to detect miRNA expression according to the manufacturer's protocols, and U6 was used as the internal reference. The relative expression of CHMP4C or miR-543 was calculated using the $2^{-\Delta\Delta Cq}$ method (11). The sequences of the primers used were as follows: CHMP4C, 5'-GAGAAGCCCTGGAGAAC-3' (forward) and 5'-CACCAAAGCCAACCC-3' (reverse); 18S, 5'-CTTAGTTGGTGGAGCGATTTGTC-3' (forward) and 5'-CGGACATCTAAGGGCATCACA-3' (reverse); miR-543, 5'-GAGAAGTTGCCCGTGTT-3' (forward) and 5'-CGCGAATGTTTCGTCA-3' (reverse); and U6, 5'-CGCTTCGGCAGCACATATAC-3' (forward) and 5'-AAATATGGAACGCTTCACGA-3' (reverse).

Western blotting. SiHa and HeLa cell proteins were extracted using RIPA lysis buffer (Shanghai Bestbio Biotechnology Co., Ltd,) after transfection, and protein determination was performed by the BCA method. Proteins of different molecular weights were separated using 10% SDS-PAGE in which 40 μg protein was loaded to each lane, and subsequently electrotransferred to Hybond membranes (MilliporeSigma; Merck KGaA). Subsequently, 3% BSA (BEIJING SOLARBIO TECHNOLOGY CO., LTD) was used to block non-specific sites at room temperature for 2 h, and anti-CHMP4C (1:1,000; #16256-1-AP; Proteintech Group, Inc.), anti-Bcl-XL (1:2,000; #10783-1-AP; Proteintech Group, Inc.), anti-Bcl2 (1:500; #66799-1-Ig; Proteintech Group, Inc.), anti-Survivin (1:1,000; #10508-1-AP; Proteintech Group, Inc.), anti-Caspase-7 (1:1,000; #27155-1-AP; Proteintech Group, Inc.) and anti-HPV16/18 E6 (1:50; #sc-460; Santa Cruz Biotechnology, Inc.) antibodies were added and incubated overnight at 4˚C. Anti-β-actin (1:10,000; #66009-1-Ig; Proteintech Group, Inc.), GAPDH (1:1,000; #60004-1-Ig; Proteintech Group, Inc.) or anti-α-tubulin (1:1,000; #80762-1-RR; Proteintech Group, Inc.) antibodies were used as controls. On the second day, the membrane was incubated with anti-rabbit IgG (1:10,000; cat. no. #SA00001-2; Proteintech Group, Inc.) or anti-mouse (1:10,000; #SA00001-1; Proteintech Group, Inc.) antibodies at room temperature for 2 h. The protein bands were visualized using the Enhanced Chemiluminescence kit (SuperSignal™ West Pico PLUS Chemiluminescence substrate; Thermo Fisher Scientific, Inc.).

Data analysis. SPSS 24.0 software (IBM Corp.) was used to perform the statistical analysis. All data are expressed as the mean ± standard deviation. The immunohistochemistry results were analyzed using Fisher's exact test. Comparisons between the experimental and control groups were performed using an unpaired double-tailed t-test, and multiple groups were compared using one-way ANOVA and Dunnett's posttest. $P<0.05$ was considered to indicate a statistically significant difference.

Results

Characteristics of CHMP4C in the tumorigenesis of cervical cancer. Bioinformatics analysis was used to assess the role of CHMP4C in cervical cancer. The GEPIA database and log-rank tests demonstrated that a higher CHMP4C expression may have a worse clinical prognosis than those with a lower CHMP4C expression (Fig. 2A). Following this, immunohistochemistry was performed using normal cervical and cervical cancer tissues to further assess the expression of CHMP4C in cervical cancer.

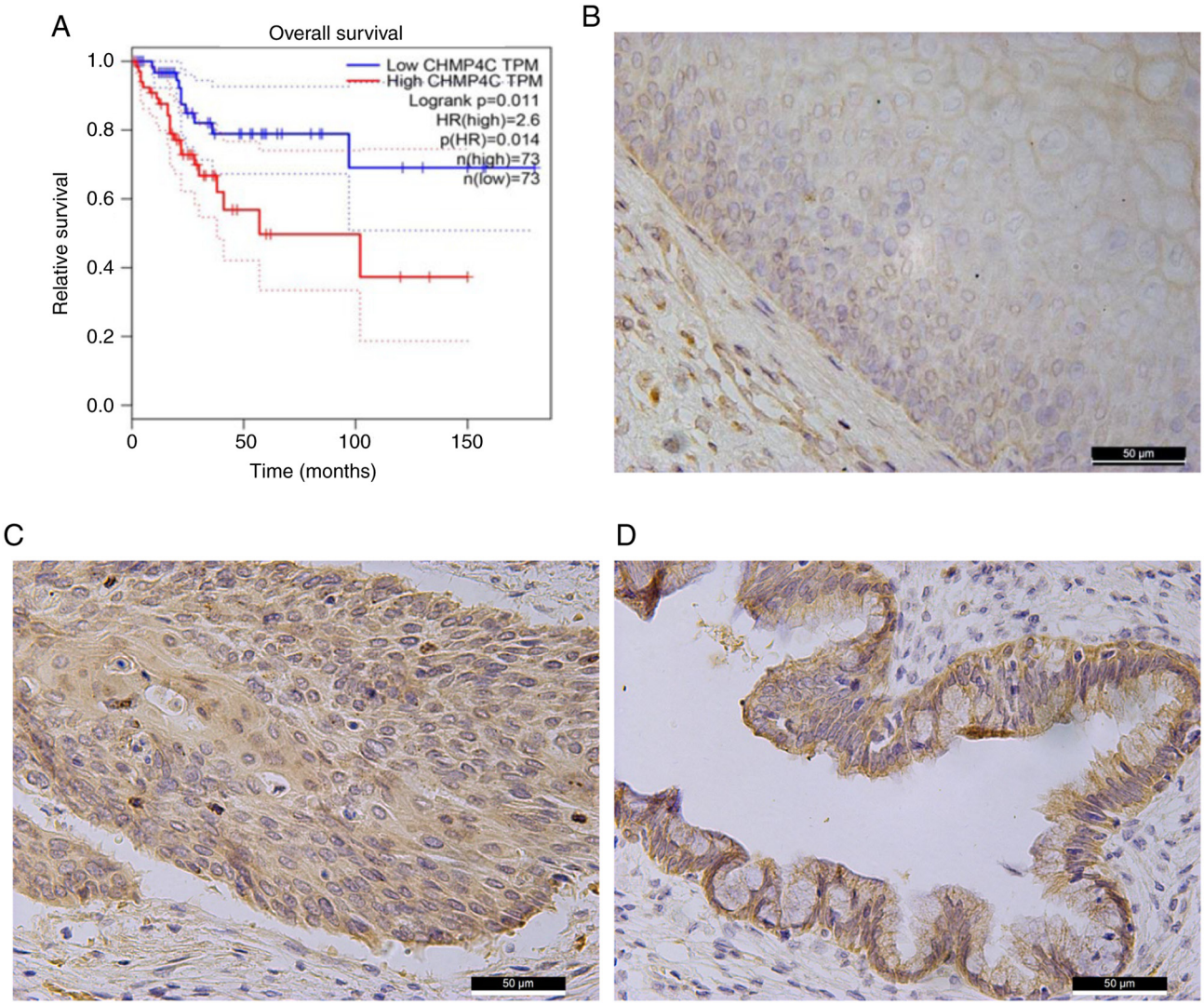

Figure 2. Influence of CHMP4C expression on the occurrence and development of cervical cancer. (A) Kaplan-Meier analyses of the overall survival rate of patients with cervical squamous cell carcinoma and endocervical adenocarcinoma with high or low expression of CHMP4C, derived from the Gene Expression Profiling Interactive Analysis database. Representative immunohistochemical staining of cervical cancer tissues for CHMP4C expression: (B) Normal tissues showed weak immunostaining, (C) squamous cell carcinoma tissues showed strong immunostaining, and (D) adenocarcinoma tissue showed strong immunostaining. CHMP4C, charged multivesicular body protein 4C; TPM, transcripts per million; HR, hazard ratio.

The results revealed that the expression level of CHMP4C in malignant cervical tumor tissues was significantly higher than that in normal tissues (Fig. 2B-D; Table SI; P<0.05). This finding indicates that CHMP4C may participate in cervical cancer tumorigenesis. Moreover, the level of CHMP4C was positively associated with the age of the patients (Table SII; P<0.05).

Effect of CHMP4C expression on the phenotype of cervical cancer cells. Firstly, expression of CHMP4C in each HPV-positive cervical cancer cell line was detected using RT-qPCR, and SiHa and HeLa cells were selected as the experimental objects as they had the highest expression of CHMP4C out of the cervical cancer cell lines assessed (Fig. 3A). Furthermore, western blotting demonstrated that the expression level of CHMP4C was significantly higher in cervical cancer SiHa and HeLa cells compared with that in the normal cervical H8 cells (Fig. 3B).

To evaluate the biological function of CHMP4C, SiHa and HeLa cells were transfected with si-CHMP4C or si-Scramble, and the transfection efficiency was determined using RT-qPCR. The results demonstrated that the expression level of CHMP4C significantly decreased following siRNA transfection, compared with the control (Fig. 4A and B; P<0.05). Silencing of CHMP4C expression was also associated with a significant decrease in cell proliferation, compared with the control (Fig. 4C and D; P<0.05). This indicates that CHMP4C promotes cell proliferation. Moreover, the cell apoptosis assay revealed that after 48 h of transfection, the si-CHMP4C cells had a significantly higher apoptosis rate than the control cells (Fig. 4E and F; P<0.05). A significant reduction in cell migration (Fig. 4G and H; P<0.05) and invasion (Fig. 4I and J; P<0.05) was also demonstrated in cells with downregulated CHMP4C expression, in comparison with the control cells. Conversely, the plasmid was transfected in the SiHa and HeLa cells to overexpress CHMP4C and assess the transfection efficiency of the plasmid using RT-qPCR (Fig. 5A and B; P<0.05). The results revealed that, in comparison with the vector control, overexpression of CHMP4C resulted in a significant

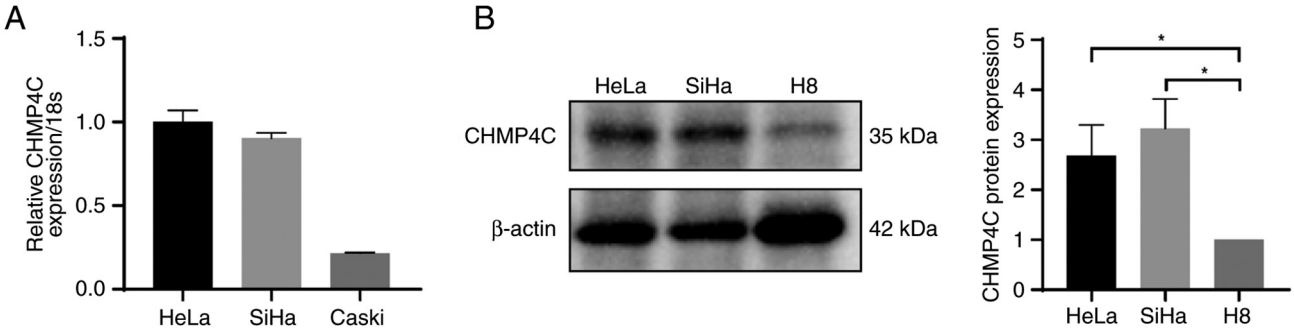

Figure 3. Cell line selection and CHMP4C expression validation. (A) Expression of CHMP4C mRNA was assessed using reverse transcription-quantitative PCR in the cervical cancer SiHa, HeLa and Caski cell lines. (B) Western blotting was used to evaluate the protein expression level of CHMP4C in the cervical cancer cell lines HeLa and SiHa, and in the normal cervical H8 cell line. Experiments were repeated three times independently. *P<0.05. CHMP4C, charged multivesicular body protein 4C.

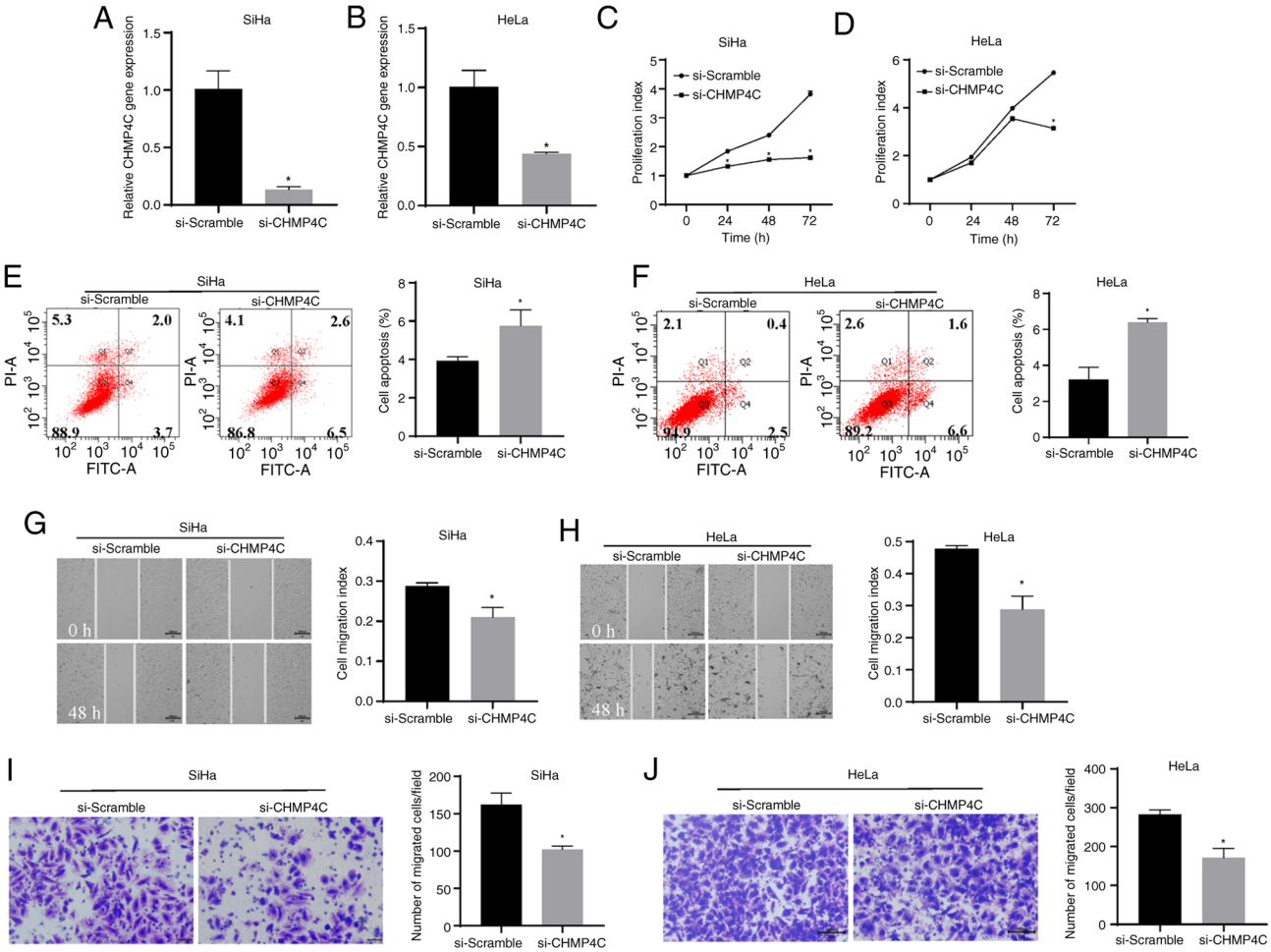

Figure 4. Assessment of si-CHMP4C transfection efficiency and the effect of silencing CHMP4C expression on cervical cancer cells. After transfection with si-CHMP4C, reverse transcription-quantitative PCR assessed the expression of CHMP4C in (A) SiHa and (B) HeLa cells. The MTT assay evaluated the effect of CHMP4C silencing on the viability of (C) SiHa and (D) HeLa cells. Flow cytometry was used to assess the effect of CHMP4C silencing on the apoptosis of (E) SiHa and (F) HeLa cells. The wound-healing assay in (G) SiHa and (H) HeLa cells, and the cell invasion assay in (I) SiHa and (J) HeLa cells evaluated cell migration and invasion, respectively, in the presence of si-CHMP4C. Experiments were repeated three times independently. *P<0.05. si, small interfering; CHMP4C, charged multivesicular body protein 4C.

increase in cell proliferation (Fig. 5C and D; P<0.05) and migration (Fig. 5E and F; P<0.05), and a significant reduction in the rate of cell apoptosis (Fig. 5G and H; P<0.05). The observed changes in phenotype indicate that CHMP4C acts as a proto-oncogene in cervical cancer cells.

CHMP4C expression is regulated by E6. The occurrence of cervical cancer is related to HPV (namely, high-risk HPV16 and HPV18) infection. Viral DNA is integrated into the host genome to encode oncogenic proteins, such as E6, which interfere with the cell cycle and apoptosis via regulation of

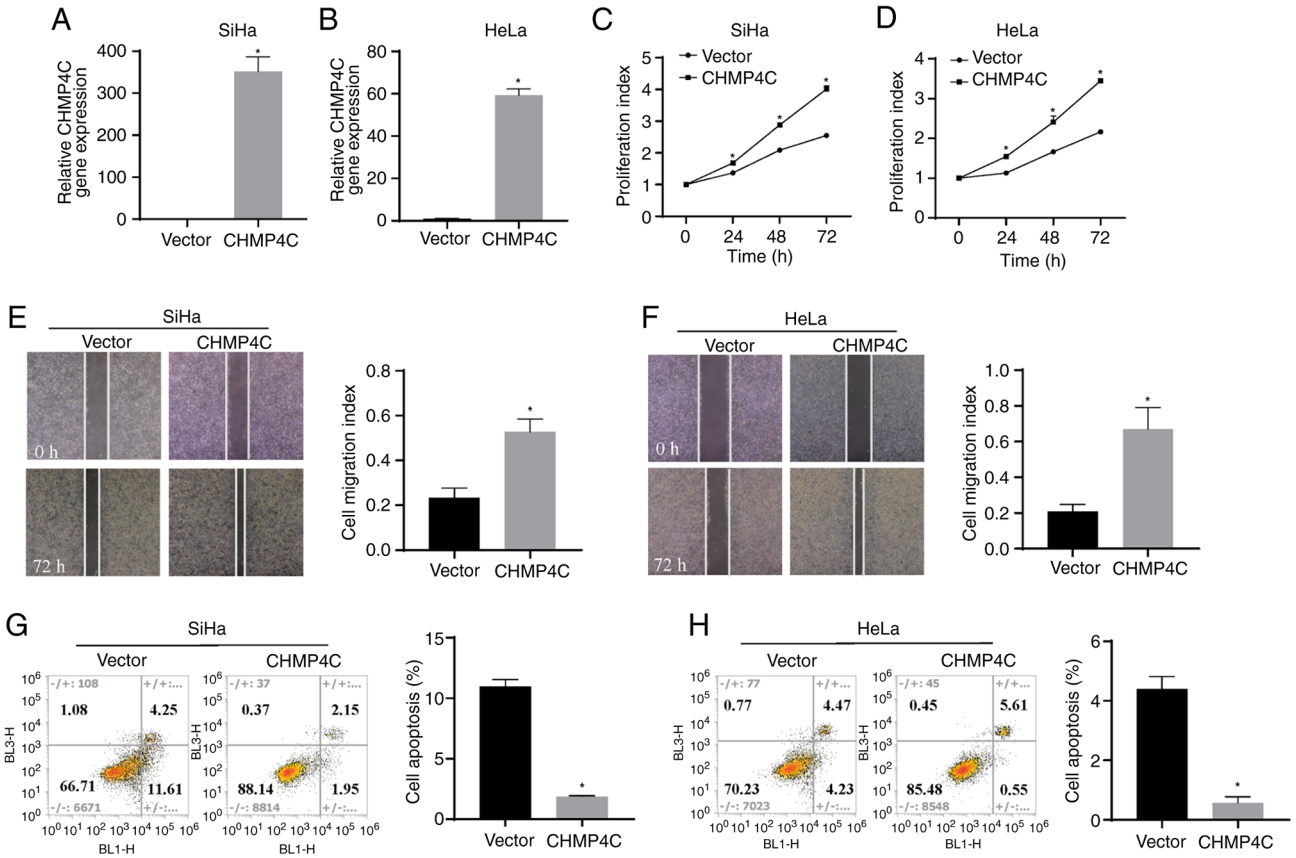

Figure 5. Evaluation of CHMP4C plasmid transfection efficiency and the effect of overexpressed CHMP4C on cervical cancer cells. The overexpression efficiency of CHMP4C in (A) SiHa and (B) HeLa cells was assessed using reverse transcription-quantitative PCR. The effect of CHMP4C overexpression on the proliferation of (C) SiHa and (D) HeLa cells was evaluated using MTT assays. The effect of the overexpression of CHMP4C on the migration of (E) SiHa and (F) HeLa cells was evaluated using wound healing assays. Flow cytometry was used to assess the effect of the overexpression of CHMP4C on the apoptotic rate of (G) SiHa and (H) HeLa cells. Experiments were repeated three times independently, *P<0.05. CHMP4C, charged multivesicular body protein 4C.

Bcl2 and Bcl-XL (12-14). Western blotting showed that the expression of Bcl2, Bcl-xL, and Survivin was decreased when CHMP4C expression was silenced, but Caspase-7 expression was increased (Fig. 6A). Therefore, CHMP4C increased the susceptibility of cervical cancer through the regulation of Bcl2, Bcl-XL, Survivin and Caspase-7. Furthermore, to determine whether CHMP4C expression was associated with cervical HPV infection, HPV16 E6 expression was silenced in SiHa cells, and HPV18 E6 expression was silenced in HeLa cells through siRNA transfection. This resulted in a significant decrease in the expression of CHMP4C, compared with the controls (Fig. 6B-D; P<0.05), and demonstrated that HPV infection may lead to increased expression of CHMP4C.

miR-543 directly targets CHMP4C. E6 induction of the expression of CHMP4C was assessed. A previous study reported that E6 could inhibit miR-543 expression in human foreskin keratinocytes (HFKs) (15). Accordingly, the findings of the present study demonstrated significant increases in miR-543 expression after E6 siRNA transfection in cervical cancer cells, compared with that of the controls (Fig. 7A and B; P<0.05). Moreover, the results of bioinformatics analysis revealed that miR-543 could bind with the 3'-UTR of CHMP4C (Fig. 7C). In addition, the dual-luciferase reporter assay demonstrated that the relative luciferase activity was significantly reduced in the group co-transfected with wild-type CHMP4C 3'-UTR and miR-543, compared with that of the control groups (Fig. 7D; P<0.05). These results imply that miR-543 directly targets the 3'-UTR of CHMP4C. Furthermore, after overexpression of miR-543 by transfection of the miR-543 mimics in SiHa and HeLa cells, western blotting indicated that CHMP4C expression was significantly reduced compared with that in control cells (Fig. 7E-G; P<0.05).

Discussion

The abscission checkpoint can inhibit the abscission of cells with spindle-midzone defects and the lagging chromosomes promote CHMP4C phosphorylation by Aurora B. This affects its activity, leading to the failure of cytokinesis (16,17). It has been reported that radiation induces the expression of Aurora B and CHMP4C in non-small cell lung cancer cells, thereby maintaining cell cycle checkpoints and cell viability, and resisting apoptosis. Inhibition of CHMP4C was reported to promote the proliferation of cancer cells by inhibiting DNA repair by reducing phosphorylated H2A histone family member X and p53-binding protein 1 (53BP1) foci reacting to radiation stress (18). It has also been reported that the absence of CHMP4C-dependent abscission checkpoints increases the accumulation of 53BP1-associated DNA damage foci (6). The role of CHMP4C has received increasing attention in the field of cancer research. Pharoah *et al* (19) implicated CHMP4C as the most likely susceptibility gene candidate in the 8q21 locus of a new locus associated with the risk of epithelial

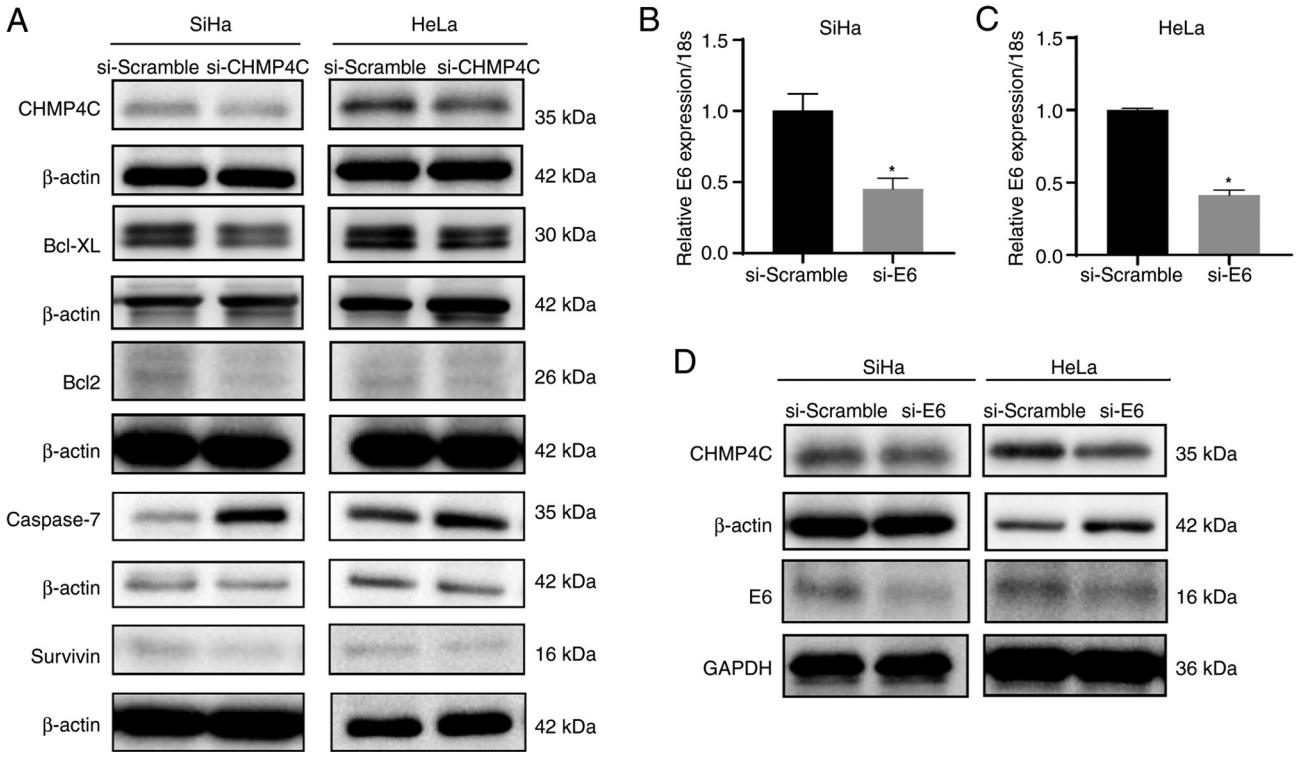

Figure 6. Effect of CHMP4C and E6 silencing on the expression of Bcl2, Bcl-XL, survivin and Caspase-7 proteins in cervical cancer cells. (A) Western blotting assessed the effect of silencing of CHMP4C expression on the expression of the apoptosis-related proteins Bcl2, Bcl-XL, Survivin and Caspase-7. Evaluation of CHMP4C knockdown using reverse transcription-quantitative PCR in (B) SiHa and (C) HeLa cells. (D) Effect of the knockdown of HPV16 E6 in SiHa cells and HPV18 E6 in HeLa cells on the expression of CHMP4C. The experiments were repeated three times independently. $^{*}P<0.05$. CHMP4C, charged multivesicular body protein 4C; HPV, human papillomavirus; si, small interfering.

ovarian cancer. Moreover, human CHMP4C polymorphisms also increase the risk of prostate and skin cancer (8).

With regards to the relationship between CHMP4C and cervical cancer, the immunohistochemistry results of the present study demonstrated that the expression level of CHMP4C was higher in cervical cancer tissues compared with normal tissues. Analysis of the GEPIA database revealed that cervical cancer is associated with a poor clinical prognosis due to the increased expression of CHMP4C. Accordingly, in the present study, CHMP4C silencing in SiHa and HeLa cells resulted in a reduction in the level of cell proliferation, migration and invasion, and an increase in the rate of apoptosis. Conversely, CHMP4C overexpression had the opposite effect on cell proliferation, cell migration and apoptosis. In addition, silencing of CHMP4C reduced the level of Bcl2, Bcl-XL and Survivin expression, and increased the expression level of Caspase-7. The process of apoptosis involves several genes, including those of the Bcl-2 family, the caspase family and the inhibitor of apoptosis proteins (IAP) family (20). The Bcl2 protein family is the key to the regulation and execution of mitochondrial-mediated intrinsic apoptosis, among which Bcl2 and Bcl-XL belong to a group of pro-survival proteins (21,22). Moreover, studies have revealed that the expression of Bcl2 may be associated with the development of cervical cancer and provide prognostic information (22,23). Survivin is a member of the IAP family of proteins and inhibits apoptosis by binding directly to Caspase-3 and Caspase-7 of the caspase family to inhibit their activity (24). It is overexpressed in many cancers and serves an important role in promoting tumor cell proliferation, progression, angiogenesis, therapeutic resistance and poor prognosis (25). A previous study also reported that overexpression of CHMP4C in cervical cancer cells accelerates cell migration and invasion by activating epithelial-mesenchymal transition (26). The aforementioned results demonstrate that CHMP4C increases the susceptibility of cervical cancer and promotes tumorigenesis and progression of cervical cancer.

Infection with HPV is the underlying cause of invasive cervical cancer (27-29). Viral DNA is integrated into the host genome to encode the oncogenic E6 and E7 proteins. E6 and E7 can interfere with cell cycle and apoptosis, which are critical factors in cellular transformation and carcinogenesis (12,13). Therefore, occurrence of cervical cancer is related to HPV infection, and CHMP4C increases the susceptibility to cervical cancer. To determine whether CHMP4C was related to cervical HPV infection, the present study knocked down E6 expression in cervical cancer cells and the results revealed that the expression of CHMP4C was decreased in the E6-knockdown cells. Thus, the E6 protein encoded by the HPV during cervical infection may regulate CHMP4C expression.

According to a previous report, miR-543 expression decreases after HPV16 E6 expression increased in HFKs (15). miRNAs are non-protein-encoding RNAs with a length of ~21 nucleotides. They inhibit the expression of their target genes primarily through interaction with the corresponding 3'-UTR of the mRNA, thereby regulating biological events, including cell proliferation, differentiation and apoptosis (30,31). Moreover, miRNA dysregulation is associated with the occurrence,

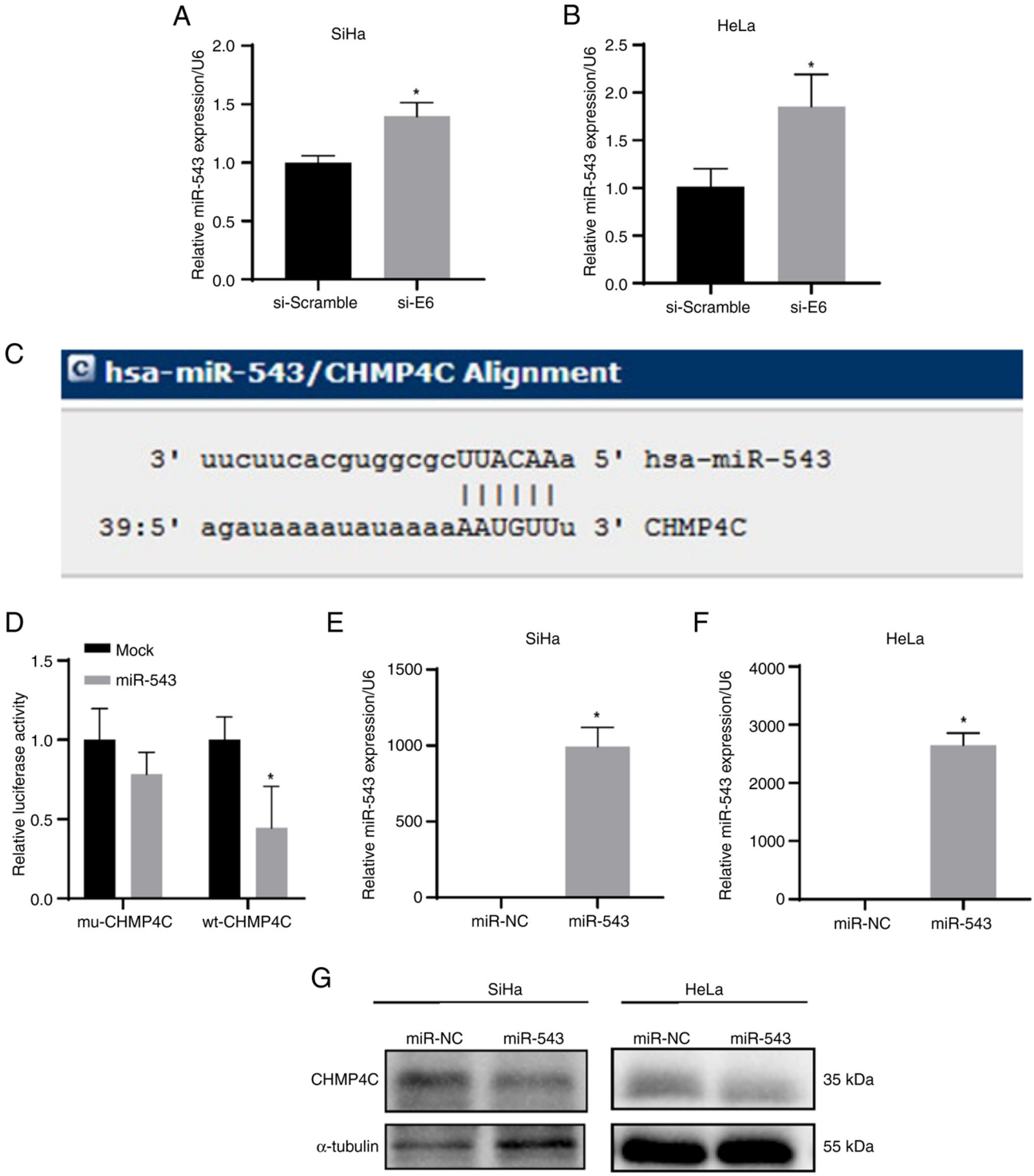

Figure 7. CHMP4C as a direct target of miR-543. Effect of the knockdown of (A) HPV16 E6 in SiHa cells and (B) HPV18 E6 in HeLa cells on the expression of miR-543. (C) Bioinformatics analysis results for a potential binding site between miR-543 and CHMP4C. (D) The dual-luciferase reporter assay was used to assess the effect of the overexpression of miR-543 on the luciferase activity of 293T cells transfected with wtCHMP4C. The overexpression efficiency of miR-543 mimics was assessed using reverse transcription-quantitative PCR in (E) SiHa and (F) HeLa cells. (G) Effect of the overexpression of miR-543 on the expression of CHMP4C was evaluating using western blotting. The experiments were repeated three times independently. *P<0.05. CHMP4C, charged multivesicular body protein 4C; miR, microRNA; mu, mutant; wt, wild-type; si, small interfering; NC, negative control; HPV, human papillomavirus.

development, metastasis and drug resistance to cancer (32). Bioinformatics analysis revealed a potential connection site between the 3'-UTR of CHMP4C and miR-543, and this implies that E6 may regulate CHMP4C expression through miR-543. After E6 was knocked down in SiHa and HeLa cells, the expression level of miR-543 was elevated. Meanwhile, elevated miR-543 expression was associated with reduced CHMP4C expression. Moreover, the dual-luciferase reporter assay demonstrated that CHMP4C was the target of miR-543. In addition, studies have reported that miR-543 expression is decreased in cervical cancer, and its expression level is associated with tumor size, FIGO stage and lymph node metastasis.

In line with the results of the present study, miR-543 is known to inhibit tumor cell proliferation, invasion and migration, and also promote apoptosis, thereby inhibiting the development of cervical cancer (33). Based on these findings, we hypothesize that CHMP4C promotes the progression of cervical cancer through the HPV E6/miR-543 axis.

In conclusion, the present research indicates that the HPV-encoded E6 oncoprotein may reduce the expression level of miR-543 and relieve the inhibitory effect of miR-543 on CHMP4C. By contrast, high expression level of CHMP4C may inhibit apoptosis by regulating Bcl2, Bcl-XL, Survivin and Caspase-7 expression, thereby promoting the tumorigenesis and progression of cervical cancer.

Acknowledgements

Not applicable.

Funding

The present research was supported by Guangdong Medical Science and Technology Research (grant no. A2023337), the Guangzhou Science and Technology Project (grant nos. 202 4A03J0182 and 2023A03J0375) and the Clinical High-tech and Major Technology Projects in Guangzhou (grant no. 2024PL-ZD06).

Availability of data and materials

The data generated in the present study may be requested from the corresponding author.

Authors' contributions

RCL, YMJ, JH, YPD, YMZ and XJS conceived the study and wrote the manuscript. RCL, YMJ, JH, YPD and YMZ performed the experiments. RCL, YMJ and JH analyzed the data. RCL and XJS confirmed the authenticity of all the raw data. All authors read and approved the final manuscript.

Ethics approval and consent to participate

The present study was approved by the Ethics Committee of the Third Affiliated Hospital Guangzhou Medical University (approval no. 2019-037). Written informed consent was obtained from all individual participants included in the study.

Patient consent for publication

Not applicable.

Competing interests

The authors declare that they have no competing interests.

References

1. Bray F, Laversanne M, Sung H, Ferlay J, Siegel RL, Soerjomataram I and Jemal A: Global cancer statistics 2022: GLOBOCAN estimates of incidence and mortality worldwide for 36 cancers in 185 countries. CA Cancer J Clin 74: 229-263, 2024.
2. World Health Organization (WHO): International agency for research on cancer. Global Cancer Observatory: Cancer Today. WHO, Geneva, 2022. https://gco.iarc.who.int/media/globocan/factsheets/populations/160-china-fact-sheet.pdf. Accessed March 10, 2025.
3. Bao H, Zhang L, Wang L, Zhang M, Zhao Z, Fang L, Cong S, Zhou M and Wang L: Significant variations in the cervical cancer screening rate in China by individual-level and geographical measures of socioeconomic status: A multilevel model analysis of a nationally representative survey dataset. Cancer Med 7: 2089-2100, 2018.
4. Small W Jr, Bacon MA, Bajaj A, Chuang LT, Fisher BJ, Harkenrider MM, Jhingran A, Kitchener HC, Mileshkin LR, Viswanathan AN and Gaffney DK: Cervical cancer: A global health crisis. Cancer 123: 2404-2412, 2017.
5. Cohen PA, Jhingran A, Oaknin A and Denny L: Cervical cancer. Lancet 393: 169-182, 2019.
6. Jones PA and Baylin SB: The epigenomics of cancer. Cell 128: 683-692, 2007.
7. Carlton JG, Caballe A, Agromayor M, Kloc M and Martin-Serrano J: ESCRT-III governs the Aurora B-mediated abscission checkpoint through CHMP4C. Science 336: 220-225, 2012.
8. Sadler JBA, Wenzel DM, Williams LK, Guindo-Martínez M, Alam SL, Mercader JM, Torrents D, Ullman KS, Sundquist WI and Martin-Serrano J: A cancer-associated polymorphism in ESCRT-III disrupts the abscission checkpoint and promotes genome instability. Proc Natl Acad Sci USA 115: E8900-E8908, 2018.
9. Nikolova DN, Doganov N, Dimitrov R, Angelov K, Low SK, Dimova I, Toncheva D, Nakamura Y and Zembutsu H: Genome-wide gene expression profiles of ovarian carcinoma: Identification of molecular targets for the treatment of ovarian carcinoma. Mol Med Rep 2: 365-384, 2009.
10. Fujita K, Kume H, Matsuzaki K, Kawashima A, Ujike T, Nagahara A, Uemura M, Miyagawa Y, Tomonaga T and Nonomura N: Proteomic analysis of urinary extracellular vesicles from high Gleason score prostate cancer. Sci Rep 7: 42961, 2017.
11. Livak KJ and Schmittgen TD: Analysis of relative gene expression data using real-time quantitative PCR and the 2(-Delta Delta C(T)) method. Methods 25: 402-408, 2001.
12. Tommasino M: The human papillomavirus family and its role in carcinogenesis. Semin Cancer Biol 26: 13-21, 2014.
13. Narisawa-Saito M and Kiyono T: Basic mechanisms of high-risk human papillomavirus-induced carcinogenesis: Roles of E6 and E7 proteins. Cancer Sci 98: 1505-1511, 2007.
14. Miyashita T, Krajewski S, Krajewska M, Wang HG, Lin HK, Liebermann DA, Hoffman B and Reed JC: Tumor suppressor p53 is a regulator of bcl-2 and bax gene expression in vitro and in vivo. Oncogene 9: 1799-1805, 1994.
15. Harden ME, Prasad N, Griffiths A and Munger K: Modulation of microRNA-mRNA target pairs by human papillomavirus 16 oncoproteins. mBio 8: e02170-16, 2017.
16. Norden C, Mendoza M, Dobbelaere J, Kotwaliwale CV, Biggins S and Barral Y: The NoCut pathway links completion of cytokinesis to spindle midzone function to prevent chromosome breakage. Cell 125: 85-98, 2006.
17. Capalbo L, Montembault E, Takeda T, Bassi ZI, Glover DM and D'Avino PP: The chromosomal passenger complex controls the function of endosomal sorting complex required for transport-III Snf7 proteins during cytokinesis. Open Biol 2: 120070, 2012.
18. Li K, Liu J, Tian M, Gao G, Qi X, Pan Y, Ruan J, Liu C and Su X: CHMP4C disruption sensitizes the human lung cancer cells to irradiation. Int J Mol Sci 17: 18, 2015.
19. Pharoah PD, Tsai YY, Ramus SJ, Phelan CM, Goode EL, Lawrenson K, Buckley M, Fridley BL, Tyrer JP, Shen H, *et al*: GWAS meta-analysis and replication identifies three new susceptibility loci for ovarian cancer. Nat Genet 45: 362-370, 370e1-2, 2013.
20. Yang Y and Yu X: Regulation of apoptosis: The ubiquitous way. FASEB J 17: 790-799, 2003.
21. Chipuk JE, Moldoveanu T, Llambi F, Parsons MJ and Green DR: The BCL-2 family reunion. Mol Cell 37: 299-310, 2010.
22. Ter Harmsel B, Smedts F, Kuijpers J, Jeunink M, Trimbos B and Ramaekers F: BCL-2 immunoreactivity increases with severity of CIN: A study of normal cervical epithelia, CIN, and cervical carcinoma. J Pathol 179: 26-30, 1996.
23. Dimitrakakis C, Kymionis G, Diakomanolis E, Papaspyrou I, Rodolakis A, Arzimanoglou I, Leandros E and Michalas S: The possible role of p53 and bcl-2 expression in cervical carcinomas and their premalignant lesions. Gynecol Oncol 77: 129-136, 2000.

24. Shin S, Sung BJ, Cho YS, Kim HJ, Ha NC, Hwang JI, Chung CW, Jung YK and Oh BH: An anti-apoptotic protein human survivin is a direct inhibitor of caspase-3 and -7. Biochemistry 40: 1117-1123, 2001.
25. Chen X, Duan N, Zhang C and Zhang W: Survivin and tumorigenesis: Molecular mechanisms and therapeutic strategies. J Cancer 7: 314-323, 2016.
26. Lin SL, Wang M, Cao QQ and Li Q: Chromatin modified protein 4C (CHMP4C) facilitates the malignant development of cervical cancer cells. FEBS Open Bio 10: 1295-1303, 2020.
27. Crosbie EJ, Einstein MH, Franceschi S and Kitchener HC: Human papillomavirus and cervical cancer. Lancet 382: 889-899, 2013.
28. Muñoz N, Bosch FX, de Sanjosé S, Herrero R, Castellsagué X, Shah KV, Snijders PJ and Meijer CJ; International Agency for Research on Cancer Multicenter Cervical Cancer Study Group: Epidemiologic classification of human papillomavirus types associated with cervical cancer. N Engl J Med 348: 518-527, 2003.
29. Smith JS, Lindsay L, Hoots B, Keys J, Franceschi S, Winer R and Clifford GM: Human papillomavirus type distribution in invasive cervical cancer and high-grade cervical lesions: A meta-analysis update. Int J Cancer 121: 621-632, 2007.
30. Krol J, Loedige I and Filipowicz W: The widespread regulation of microRNA biogenesis, function and decay. Nat Rev Genet 11: 597-610, 2010.
31. Davis BN and Hata A: Regulation of MicroRNA biogenesis: A miRiad of mechanisms. Cell Commun Signal 7: 18, 2009.
32. Acunzo M, Romano G, Wernicke D and Croce CM: MicroRNA and cancer-a brief overview. Adv Biol Regul 57: 1-9, 2015.
33. Liu X, Gan L and Zhang J: miR-543 inhibites cervical cancer growth and metastasis by targeting TRPM7. Chem Biol Interact 302: 83-92, 2019.